JOURNAL OF VIROLOGY, Mar. 2008, p. 2120–2129 Vol. 82, No. 5
0022-538X/08/$08.00+0 doi:10.1128/JVI.02053-07

Cellular Determinants of Hepatitis C Virus Assembly, Maturation, Degradation, and Secretion▽

Pablo Gastaminza,[1] Guofeng Cheng,[1] Stefan Wieland,[1] Jin Zhong,[1]† Wei Liao,[2] and Francis V. Chisari[1]*

Division of Experimental Pathology, Department of Molecular and Experimental Medicine, The Scripps Research Institute, La Jolla, California 92037,[1] and Department of Medicine, Division of Endocrinology and Metabolism, University of California, San Diego, La Jolla, California 92093[2]

Received 16 September 2007/Accepted 3 December 2007

Intracellular infectious hepatitis C virus (HCV) particles display a distinctly higher buoyant density than do secreted virus particles, suggesting that the characteristic low density of extracellular HCV particles is acquired during viral egress. We took advantage of this difference to examine the determinants of assembly, maturation, degradation, and egress of infectious HCV particles. The results demonstrate that HCV assembly and maturation occur in the endoplasmic reticulum (ER) and post-ER compartments, respectively, and that both depend on microsomal transfer protein and apolipoprotein B, in a manner that parallels the formation of very-low-density lipoproteins (VLDL). In addition, they illustrate that only low-density particles are efficiently secreted and that immature particles are actively degraded, in a proteasome-independent manner, in a post-ER compartment of the cell. These results suggest that by coopting the VLDL assembly, maturation, degradation, and secretory machinery of the cell, HCV acquires its hepatocyte tropism and, by mimicry, its tendency to persist.

Hepatitis C virus (HCV) establishes persistent infection in >70% of infected individuals (25), and over 170 million people are persistently infected worldwide. Persistent HCV infection is associated with a chronic inflammatory disease (hepatitis) that ultimately leads to hepatic fibrosis, cirrhosis, and hepatocellular carcinoma (25). Chronic infection is also associated with disorders of lipid metabolism (54), with abnormal accumulation of lipids in the liver parenchymal cells (steatosis) and reduced serum beta-lipoprotein levels (52). Currently, the only approved antiviral therapy for HCV is the administration of type I interferon combined with ribavirin. However, this therapy is toxic and is effective in only a fraction of cases (43).

HCV is the sole member of the genus *Hepacivirus*, which belongs to the *Flaviviridae* family. The virus is enveloped, and the single-stranded positive-strand RNA genome contains a single open reading frame flanked by untranslated regions (5′ UTR and 3′ UTR) that contain RNA sequences essential for RNA translation and replication (17, 18). Translation of the single open reading frame is driven by an internal ribosomal entry site (IRES) sequence present within the 5′ UTR (24), and the resulting polyprotein, of approximately 3,000 amino acids in length, is processed by cellular and viral proteases into its individual components (44). The nonstructural proteins NS3, NS4A, NS4B, NS5A, and NS5B are sufficient to support efficient HCV RNA replication in membranous compartments in the cytosol (10, 35, 39). Overexpression of the core, E1, and E2 proteins is sufficient for the formation of virus-like structures in insect cells (6), and expression of the viral polyprotein leads to the formation of virus-like particles in HeLa (38) and Huh-7 (23) cells. It has been proposed that infectious particles are assembled when genomic RNA-containing core particles bud through the endoplasmic reticulum (ER) membrane (47), acquiring the viral envelope and surface glycoproteins (14, 15, 48). However, it is currently unknown how the viral particles are transported from the ER through the secretory pathway.

In infected individuals, HCV particles circulate as low-density lipoprotein (LDL)–virus complexes (3) characterized by very-low-to-low buoyant densities (from <1.03 to 1.25 g/ml), depending on the stage of the infection at which the sample is obtained (12, 46). These LDL-virus particles are rich in triglycerides and contain HCV RNA, core protein, and apolipoproteins B and E (apoB and apoE) (3), which are components of the beta-lipoproteins (very-low-density lipoproteins [VLDL] and LDL) (11). Hepatic assembly and secretion of VLDL particles play an essential role in the delivery of lipids to extrahepatic tissues (20). VLDL assembly requires the structural protein apoB, and the intraluminal ER microsomal transfer protein (MTP) (a schematic diagram of the VLDL assembly and secretion pathway is available at http://www.scripps.edu/~gastamin/Gastaminza_JVI/Suppl_Fig_1.tif) (reviewed in reference 8) facilitates two concerted processes necessary for VLDL assembly, i.e., cotranslational translocation of nascent apoB across the ER membrane and facilitated folding and transfer of lipids (8). The latter occurs in a two-step process, the first of which is required for the formation of high-density (~1.18 g/ml) VLDL precursors (21, 49), while the second yields mature VLDL particles (<1.006 g/ml) that are secreted by the cell (22). Interruption of any of these coordinated processes aborts VLDL assembly, causing apoB to be degraded cotranslationally by a ubiquitin-dependent proteasome pathway (7, 33).

* Corresponding author. Mailing address: The Scripps Research Institute, Maildrop SBR-10, 10550 North Torrey Pines Road, La Jolla, CA 92037. Phone: (858) 784-8228. Fax: (858) 784-2160. E-mail: fchisari@scripps.edu.

† Present address: Viral Hepatitis Unit, Institut Pasteur-Shanghai, 225 South Chongqing Rd., Shanghai, China 200025.

▽ Published ahead of print on 19 December 2007.

We previously reported (19) that HCV particles secreted into the supernatants of infected cell cultures have biophysical properties similar to those of particles circulating in infected patients (42). We also reported that intracellular particles are infectious, and we found that their average buoyant density was significantly higher than that of the extracellular particles (19). These biophysical differences probably reflect differences in biochemical composition, suggesting that intracellular infectious particles undergo a maturation process that enables them to acquire the low-density configuration prior to leaving the cell (19). These results suggest an interesting parallelism between the assembly and secretion of VLDL and HCV, in that intracellular high-density precursors are transformed into low-density secreted particles prior to egress. This parallelism is reinforced by the fact that HCV particles in infected patients contain apoB and apoE (3, 42), suggesting that these components might be acquired simultaneously with cellular lipids during viral egress. In this study, we defined functional aspects of infectious viral particle assembly and secretion, demonstrating that infectious HCV particle secretion is a highly regulated process in which only a fraction of the assembled infectious particles are secreted, with the rest being targeted for nonproteasomal degradation in a post-ER compartment. Moreover, we demonstrate that apoB is a rate-limiting factor in HCV infectious particle assembly and secretion and that these processes require active MTP.

(Part of this study was communicated at the 13th International Meeting on HCV and Related Viruses, Cairns, Australia, 27 to 31 August 2006.)

MATERIALS AND METHODS

Cells and viruses. Huh-7 and Huh-7.5.1 cells were cultured as previously described (57). Replicon cells were generated as described previously (9, 35). JFH-1 virus was generated by transfection, and viral stocks were produced by infection of Huh-7 cells at a multiplicity of infection (MOI) of 0.01, as described previously (57). At day 8 to 10 postinoculation, supernatants were collected and the infectivity titer was determined as described below. The infected cells were maintained and used as persistently infected cells in secretion experiments for no more than 40 days postinfection. High-titer stocks of D183 virus (58) were prepared by infection of a Huh-7.5.1 cell subclone (clone 2) (G. Cheng, unpublished data) at a low MOI (0.01) as described previously (57). A recombinant PCR approach was used to replicate the previously described J6CF–, H77–, and Con1–JFH-1 chimeric HCV genomes (45) by replacing the corresponding JFH-1 core-NS2 region in pUC-vJFH with the corresponding sequences from J6CF, H77, and Con1. Infectious JFH-1 and chimeric viruses were produced by transfection of in vitro-synthesized genomic HCV RNA into Huh-7.5.1 cells, and virus stocks containing 10^4 to 10^5 focus-forming units (FFU)/ml were prepared as described previously (57).

Chemicals. BMS-200150 was synthesized in-house by Enrique Mann, as described previously (27). Acetyl-L-leucyl-L-leucyl-L-norleucinal (ALLN) and lactacystin were purchased from Calbiochem (San Diego, CA). MG132 was purchased from A.G. Scientific (San Diego, CA). E64 was purchased from Sigma (St. Louis, MO). Brefeldin A (BFA) (GolgiPlug; 1 mg/ml) was purchased from BD Biosciences (San Diego, CA) and used at the recommended dilution (1 μg/ml).

Lentiviral particle production and Huh-7 cell transduction. Lentiviral particles were produced in HEK-293T cells by cotransfection of plasmids encoding apoB short hairpin RNAs (shRNAs) (32) and the plasmids necessary for vesicular stomatitis virus glycoprotein-pseudotyped lentivirus production as described previously (28). Cell supernatants were collected at 36 to 48 h posttransfection. The supernatants were cleared at low speed in a countertop centrifuge (2 min at 1,500 rpm). The lentiviral particle titer was determined by end-point dilution of the supernatants and immunofluorescence in Huh-7 cells, since the transduced cells express green fluorescent protein (32).

Infections. Low-multiplicity (MOI of 0.01) infection experiments were performed as previously described (57). High-multiplicity (MOI of 5) infection experiments were performed using the cell culture-adapted D183 virus (58). Huh-7 cells were plated the day before infection into 12-well plates (Corning Incorporated, Corning, NY) at 5×10^4 cells/well. Cells were inoculated with 250 μl of a high-titer (10^6 FFU/ml) D183 virus stock. At 5 hours postinoculation, the cells were washed extensively (three times with 1 ml each) with phosphate-buffered saline (PBS) and incubated in Dulbecco's modified Eagle's medium (DMEM) containing 10% fetal calf serum (FCS) for the indicated period of time.

Secretion experiments. Persistently infected cells were generated as described above. Cells were plated in 12-well plates (Corning Incorporated, Corning, NY) at 5×10^5 cells/well, washed the following day, and preincubated with drugs for 1 h at 37°C. The cells were then washed once with PBS, replenished with DMEM–10% FCS, and incubated at 37°C for the indicated periods of time.

Intracellular and extracellular infectivity titration. The infectivity titer was determined on Huh-7 cells by end-point dilution and immunofluorescence as previously described (57). Typically, 25 μl of supernatant or cell lysate (19) was serially diluted fivefold in DMEM–10% FCS, and 100 μl was used to inoculate Huh-7 cells. Infection was examined at 72 h postinoculation by immunofluorescence, using a recombinant monoclonal human immunoglobulin G (IgG) anti-E2 antibody (C1 antibody; a gift from Dennis Burton, The Scripps Research Institute) or, for the chimeric viruses bearing structural proteins from other genotypes, a monoclonal antibody against core protein C750 (Affinity Bioreagents, Golden, CO), with the appropriate secondary Alexa 555-conjugated antibodies (Invitrogen, Carlsbad, CA).

Density gradient ultracentrifugation. Gradients were formed by equal-volume (700 μl) steps of 20%, 30%, 40%, 50%, and 60% sucrose solutions in TNE buffer (10 mM Tris-HCl, pH 8, 150 mM NaCl, 2 mM EDTA) as previously described (19). Equilibrium was reached by ultracentrifugation for 16 h at 36,000 rpm (135,000 × *g*) in an SW60Ti rotor at 4°C in a Beckman L8-80 M preparative ultracentrifuge. Twelve gradient fractions of 250 μl were collected from the top and titrated for virus infectivity as described above. The densities of the fractions were determined by measuring the mass of 100-μl aliquots of each sample.

RNA extraction and quantitation. RNAs were extracted using a modification of the GTC extraction method (13) after adding 2 μg of yeast tRNA per sample as a carrier. HCV RNA levels were determined by reverse transcription–real-time quantitative PCR (RT-qPCR), using HCV JFH-1-specific primers and normalization for glyceraldehyde-3-phosphate dehydrogenase (GAPDH) mRNA levels, as described previously (30, 57). apoB mRNA was quantitated by RT-qPCR using the primers ApoBup (5′-CTG TCA GCG CAA CCT ATG AG-3′) and ApoBlo (5′-TCT GCC GAT TAT ATT TGA ATG TCA-3′).

Protein analyses. Core levels in the supernatant were determined by enzyme-linked immunosorbent assay (ELISA) as described previously (19). apoB and albumin in the cell supernatants were measured by ELISA (Alerchek, Portland, ME, and Bethyl Laboratories, Montgomery TX, respectively). Protein ubiquitination was determined by Western blotting using anti-ubiquitin (P4D1-HRP; Santa Cruz Antibodies, Santa Cruz, CA) and anti-GAPDH (Novus Biologicals, Littleton, CO) antibodies for the loading control.

RESULTS

Intracellular infectious HCV levels reflect viral assembly and degradation by the cell. Like other members of the *Flaviviridae* family, it is believed that HCV particles are assembled in the rough ER (34). Therefore, it is possible that the intracellular infectious particles previously described in our laboratory (19) are located in ER-related compartments prior to their secretion into the extracellular milieu. In order to test this hypothesis, we studied the effect of BFA on intracellular infectious particle content. BFA, a general inhibitor of secretion, has been shown to promote the accumulation of normally secreted proteins and lipoproteins in ER-related compartments (41) and to inhibit the secretion of other *Flaviviridae* (37). Persistently HCV-infected cells were treated for 9 h with BFA (1 μg/ml), and serially diluted samples of the supernatant and the infected cells were analyzed for infectious particle content by infectivity analysis of Huh-7 cells. As expected, BFA significantly inhibited the secretion of infectious HCV particles, as shown by a strong reduction in extracellular infectivity

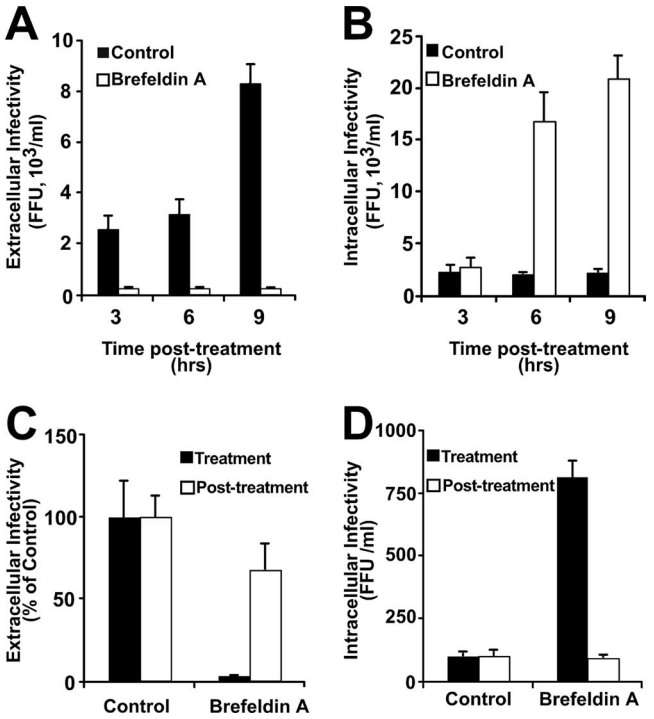

FIG. 1. BFA treatment causes intracellular accumulation of infectious HCV precursors. Persistently infected cells were treated with BFA (1 μg/ml) for 9 h at 37°C. Samples of the supernatants and cells were collected at the indicated time points, and intracellular and extracellular infectivity was determined in the absence (black bars) or presence (white bars) of BFA. (A) Extracellular infectivity (FFU/ml). (B) Intracellular infectivity (FFU/ml). (C) Persistently infected cells were treated with BFA (1 μg/ml) for a 6-h period, after which samples of supernatants were collected. Cells were washed once with PBS and further incubated for another 20 h with complete medium. Extracellular infectivity in supernatants after BFA treatment (black bars) and after drug removal (white bars) was determined by serial dilution and immunofluorescence, as described in Materials and Methods. (D) Intracellular infectivity was determined for lysates of the cells used in the experiment described for panel C. Results are presented as averages and standard deviations for triplicate experiments ($n = 3$).

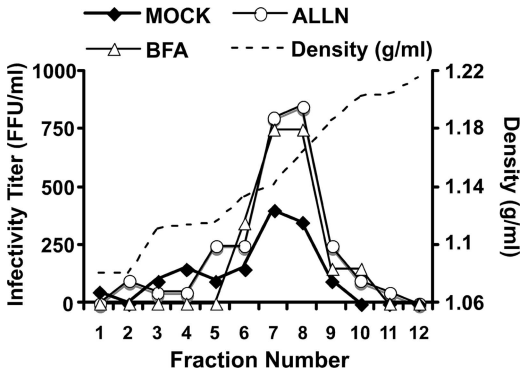

FIG. 2. Buoyant density of infectious particles accumulated within infected cells. The buoyant density profile of particles present in persistently infected cell cultures was determined by equilibrium ultracentrifugation of sucrose gradients. Cell lysates of persistently infected cells were prepared after 6 h of BFA (1 μg/ml) or ALLN (40 μM) treatment and were ultracentrifuged in an isopycnic sucrose gradient (20 to 60% sucrose) until equilibrium was reached. Fractions of the gradient were collected from the top, and infectivity was determined by serial dilution and immunofluorescence. The buoyant density profile is represented by the infectivity (FFU/ml) present in each fraction. The density (g/ml) of each fraction is shown as a dotted line.

(Fig. 1A) that was independent of residual BFA present in the diluted supernatants used in the infectivity assay (http://www.scripps.edu/~gastamin/Gastaminza_JVI/Suppl_Fig_2.tif). Interestingly, the inhibition of particle secretion coincided with a progressive accumulation of intracellular particles within the infected cells, as shown by the increasing number of infectious particles present in total cell lysates over time (Fig. 1B). HCV secretion was restored (Fig. 1C) and intracellular infectivity returned to baseline (Fig. 1D) after removal of the drug, indicating that the effect of BFA was reversible and that it did not significantly compromise the viability of the cells under these conditions. In order to determine if the accumulated intracellular particles were high-density precursors or mature low-density infectious particles whose secretion had been prevented by BFA treatment, we analyzed the buoyant density profile of these particles in isopycnic sucrose density gradients. This analysis revealed that the accumulated particles peaked at a density of 1.15 g/ml, corresponding to the density of intracellular precursors (Fig. 2, compare mock with BFA treatment) (19). Overall, these results suggest that immature (high-density) HCV particles form in the ER and that maturation into low-density particles occurs after they leave the ER.

In order to determine if intracellular HCV precursors are targeted for presecretory proteasomal degradation, similar to misfolded proteins or immature apoB-containing VLDL precursors (56), we monitored the impact of proteasome inhibitors (lactacystin, MG132, and ALLN) on steady-state HCV infectivity levels in persistently infected Huh-7 cells. Despite the fact that the three compounds profoundly inhibited proteasomal degradation of ubiquitinated proteins (Fig. 3A), only ALLN provoked accumulation of intracellular infectious particles (Fig. 3B). Sucrose gradient ultracentrifugation analyses confirmed that the intracellular particles that accumulated during ALLN treatment displayed the biophysical properties of intracellular virus precursors, with a distinct peak of buoyant density at 1.15 g/ml (Fig. 2, compare mock and ALLN treatments).

In addition to its ability to inhibit the proteasome, ALLN is also known to inhibit cysteine proteases (51). The lack of accumulation of intracellular infectivity in the presence of lactacystin and MG132 argues against a proteasomal degradation mechanism. These results suggest that either a rate-limiting component of intracellular infectious particle assembly is degraded in a nonproteasomal manner under normal conditions or that infectious intracellular precursors themselves are degraded after they are assembled. After the initial rapid accumulation (<1.5 h) of intracellular infectious particles, virus accumulation appeared to reach a plateau (Fig. 3C), which lasted for several hours (data not shown). ALLN treatment did not suppress the extracellular infectivity level compared to that of the untreated cells (Fig. 3D), suggesting that unlike BFA, ALLN does not inhibit infectious particle secretion. Analysis of infectivity after purification of the particles through a sucrose cushion confirmed that the presence of ALLN in these supernatants did not interfere with the infectivity titration assay (http://www.scripps.edu/~gastamin/Gastaminza_JVI/Suppl

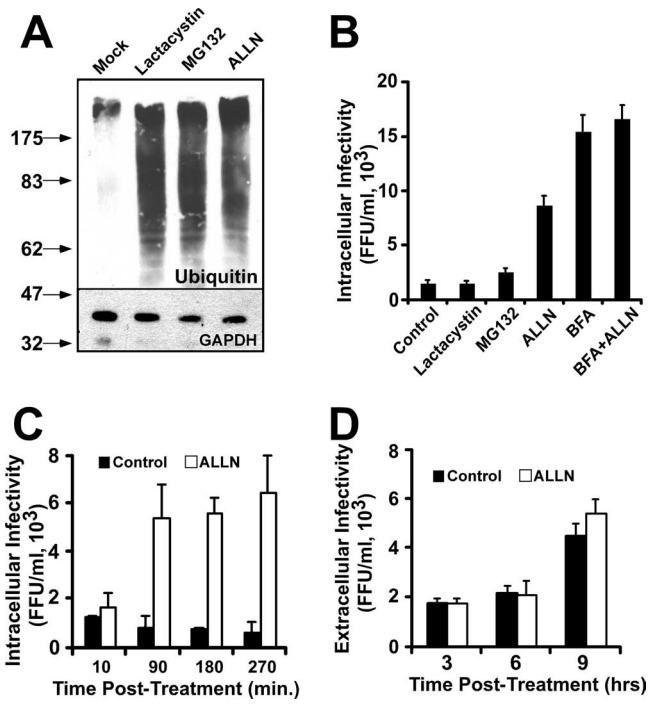

FIG. 3. Intracellular infectious HCV precursors are susceptible to nonproteasomal degradation. Persistently infected cells were treated with the proteasome inhibitors lactacystin, MG132, and ALLN (40 μM) at 37°C. (A) Inhibition of the proteasome was demonstrated by the accumulation of ubiquitinated proteins, as shown by Western blotting with anti-ubiquitin antibodies of total cell extracts obtained after a 16-h incubation period. Samples were analyzed for GAPDH content as a loading control. Molecular mass markers are shown in kilodaltons. (B) Intracellular infectivity (FFU/ml) was determined at 6 h posttreatment in the presence of lactacystin, MG132, ALLN (40 μM), or ALLN (40 μM) in combination with BFA (1 μg/ml). (C) Time course showing rapid intracellular infectious particle accumulation in the presence of ALLN (40 μM) (white bars) compared to that in the control (black bars). (D) Extracellular infectivity after treatment of persistently infected cells with 40 μM ALLN for 9 h at 37°C. Extracellular infectivity titers were determined in the presence (white bars) and absence (black bars) of the drug, as described in Materials and Methods, and are presented as averages and standard deviations for triplicate experiments ($n = 3$).

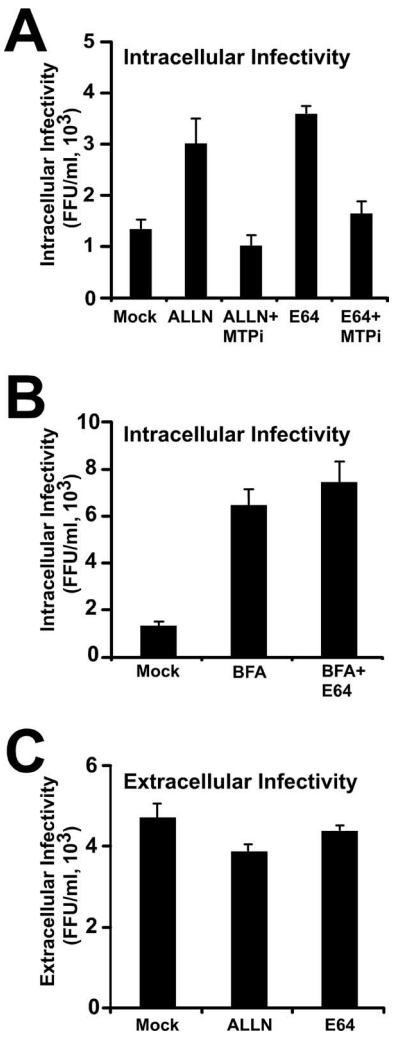

FIG. 4. E64 and ALLN prevent post-ER degradation of intracellular precursors. Persistently infected cells were incubated with E64 (25 μg/ml) and ALLN (50 μM) for 6 h at 37°C. (A) Intracellular infectious particles accumulate in the presence of E64 and ALLN, and this accumulation can be prevented by simultaneous addition of MTPi (15 μM). (B) Intracellular infectious HCV accumulation in the presence of BFA (1 μg/ml) and E64 (25 μg/ml). (C) Extracellular infectivity in the supernatants of persistently infected cells treated with E64 (25 μg/ml) or ALLN (50 μM). Results are shown as means and standard deviations for triplicate experiments ($n = 3$).

_Fig_2.tif). These results imply that the number of intracellular particles is not rate limiting for HCV secretion in persistently infected cells and that only a subset of the assembled infectious precursors are secreted, while the rest are targeted for degradation. Simultaneous treatment of the cells with ALLN and BFA did not produce an additive effect on intracellular infectious HCV accumulation (Fig. 3B), suggesting that degradation takes place in a post-ER compartment(s). Importantly, similar results were obtained with E64 (25 μg/ml) (Fig. 4), a cysteine protease inhibitor that has also been shown to protect apoB from presecretory, post-ER degradation (16, 53). These results support the notion that intracellular HCV particle content is regulated by a post-ER degradation mechanism governed by a cysteine protease. Interestingly, similar observations have been reported for apoB and apoE, which have been shown to be degraded in a post-ER compartment by a cysteine protease-dependent mechanism (1, 55). Collectively, these results imply that intracellular degradation is the default pathway for HCV precursors in persistently infected Huh-7 cells and that low-density particles escape degradation to be secreted into the extracellular milieu.

HCV particle assembly and secretion are MTP dependent. The assembly of VLDL precursors begins with the translocation of apoB into the ER lumen in a process that is facilitated by the transfer of lipids to the nascent apoB polypeptide by MTP (50). In view of the different densities of the intracellular and extracellular infectious particles, we set out to study the possibility that efficient secretion of HCV particles is dependent on MTP by using BMS-200150 (MTPi), a potent and selective MTP inhibitor (27). Treatment with MTPi (10 μM) inhibited infectious HCV particle secretion, as shown by reduced infectivity in the supernatant of the infected cells

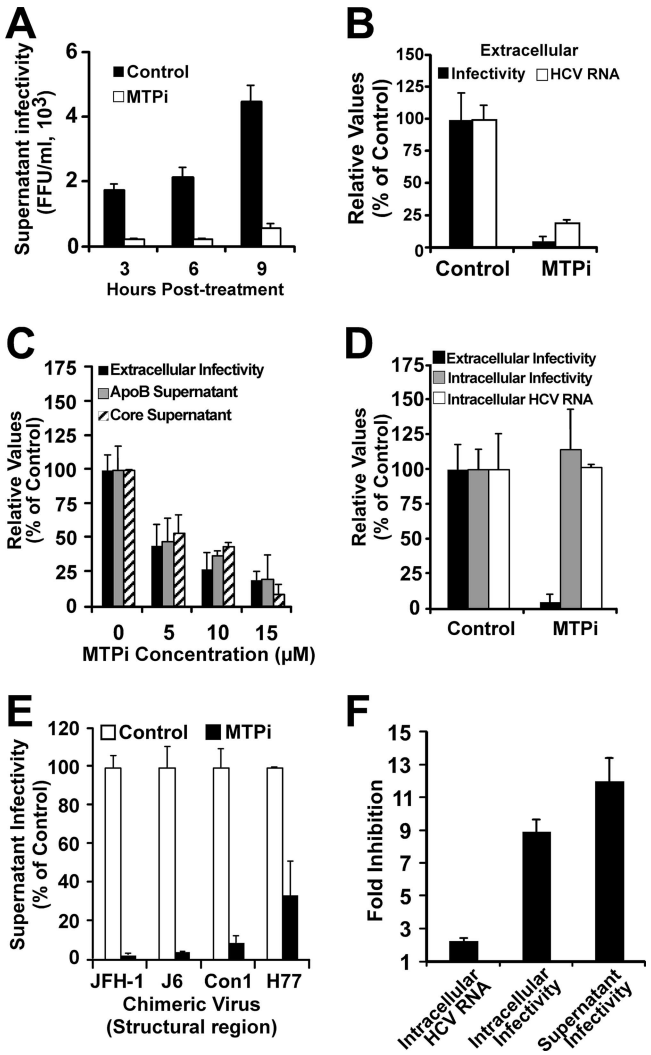

FIG. 5. Infectious HCV particle secretion inhibition by the MTP inhibitor BMS-200150. Persistently infected Huh-7 cells were treated with MTPi as described in Materials and Methods. (A) Accumulation of extracellular infectious particles was reduced in the presence of 10 μM MTPi (white bars) compared to that in cells treated with dimethyl sulfoxide (DMSO) (control) when infectivity in the supernatants was analyzed at the indicated times posttreatment. Results are shown as infectivity titers, in FFU/ml. (B) MTPi treatment (10 μM) similarly reduced both extracellular infectivity (black bars) and HCV RNA content (white bars) of infected cell supernatants collected at 8 h posttreatment, as determined by RT-qPCR. Results are shown as percentages of the control level. (C) Dose-dependent reduction of extracellular infectivity titers (black bars) in supernatants of infected cells treated with the indicated doses of MTPi collected at 8 h posttreatment. Human apoB (gray bars) and HCV core protein (hatched bars) levels were decreased proportionally, as evaluated by ELISA. Results are shown as percentages of the control level. (D) MTPi treatment did not alter either the intracellular infectious particle content (gray bars) or the intracellular level of HCV RNA (white bars), while it significantly reduced the supernatant infectivity titer (black bars). Results are shown as percentages of the control levels (DMSO). (E) Cells persistently infected with chimeric viruses bearing structural proteins corresponding to genotypes 1a (H77), 1b (Con1), and 2a (J6) were treated with MTPi (10 μM) for 9 h at 37°C. The infectivity titers after treatment were normalized to that of vehicle-treated (DMSO) cells. (F) Single-cycle infection in the presence of MTPi. Huh-7 cells were inoculated at an MOI of 5. At 5 hours postinoculation, the cells were washed once with PBS and treated with MTPi (10 μM) or vehicle (DMSO). Samples of the cells and their supernatants were collected at 24 h postinfection. Extra- and intracellular infectivity, as well as HCV RNA content, were determined as described in Materials and Methods. The results are expressed as inhibition of intracellular RNA accumulation, as determined by RT-qPCR (HCV RNA copies/μg), and intracellular and extracellular infectivity, as determined by titration (FFU/ml). Values are expressed as average levels of inhibition and standard deviations for triplicate infections ($n = 3$).

(Fig. 5A). HCV RNA analysis using RT-qPCR confirmed that the number of particles was reduced in these supernatants (Fig. 5B). Treatment of the infected cells with increasing doses of the inhibitor revealed a dose-dependent inhibition of HCV infectivity and core protein secretion that was proportional to the reduction of apoB secretion (Fig. 5C). This inhibition was specific, since normal levels of secreted human albumin were found in these supernatants, regardless of the MTPi concentration (data not shown). These results suggest that MTP inhibition reduced the ability of the infected cells to secrete HCV particles in a dose-dependent manner. Intracellular HCV RNA levels and infectivity titers remained unchanged in cells treated with the MTP inhibitor (Fig. 5D), suggesting that it specifically targeted HCV secretion. The secretion of chimeric JFH-1 viruses bearing structural proteins corresponding to genotype 1a (H77), genotype 1b (Con1), and genotype 2a (J6) was also susceptible to inhibition by MTPi (Fig. 5E). These observations, made with persistently infected cells, were confirmed in single-step infection experiments. Briefly, naive Huh-7 cells were inoculated with HCV at an MOI of 5 as described in Materials and Methods, after which they were replenished with complete medium or medium containing MTPi (10 μM). At 24 hours postinoculation, the cells and their supernatants were tested for intracellular HCV RNA and intra- and extracellular infectivity. Both intracellular and extracellular infectivity levels were significantly reduced (≈10-fold), with little or no change in the intracellular accumulation of viral RNA (Fig. 5F), indicating that MTP inhibition reduces the production of infectious intracellular HCV and its secretion into the extracellular milieu. These results suggest that in addition to promoting the secretion of infectious HCV particles, MTP either promotes the assembly of infectious intracellular HCV particles or prevents their degradation by promoting their maturation into low-density particles.

To explore these alternate possibilities, we took advantage of the fact that infectious particles accumulate in BFA-treated cells in a manner reflecting the infectious particle production rate (Fig. 1B). Thus, we studied the accumulation of intracellular infectivity in the presence of MTPi in cells treated with BFA. HCV-infected cells were simultaneously treated with BFA and MTPi (10 μM) for 8 h at 37°C. Although infectious particles accumulated intracellularly after BFA treatment alone (Fig. 6A), accumulation did not occur when the cells were cotreated with MTPi or treated with MTPi alone, suggesting that MTP inhibition impairs a process that precedes the accumulation of new infectious HCV precursors, supporting the notion that MTP is required for infectious particle assembly.

Since the steady-state level of intracellular infectious HCV particles is regulated by an ALLN-sensitive mechanism (Fig.

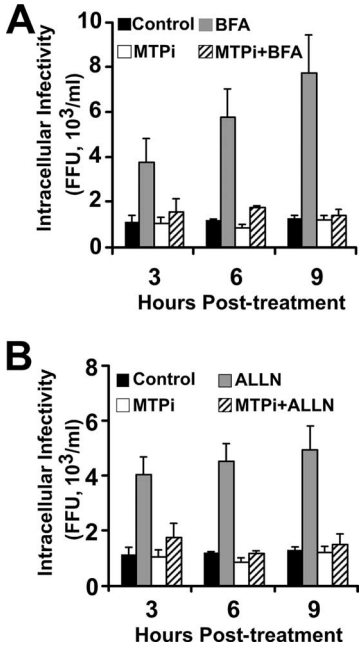

FIG. 6. MTP inhibition results in reduced intracellular HCV infectious accumulation, not in increased intracellular infectious particle degradation. (A) Persistently infected cells were treated with BFA alone (1 μg/ml) or in combination with MTPi (10 μM) for 9 h at 37°C. (B) Cells were treated with ALLN alone (40 μM) or in combination with MTPi (10 μM) for 9 h at 37°C. Cells were collected at the indicated times posttreatment, and the infectivity titers of total cell lysates were determined as described in Materials and Methods. Results are presented as averages and standard deviations for triplicate experiments ($n = 3$) and are shown as infectivity titers, in FFU/ml.

3), and since MTP inhibition increases the apoB degradation rate (7), we asked whether MTP inhibition could enhance degradation of the intracellular infectious HCV particles. Simultaneous treatment of persistently infected cells with MTPi (10 μM) and ALLN (40 μM) did not result in the accumulation of intracellular infectivity observed with ALLN treatment alone (Fig. 6B), suggesting that MTP inhibition targets a process that precedes intracellular HCV degradation, probably at the level of infectious particle assembly. Overall, these results suggest that MTP inhibition inhibits the release of HCV infectious particles into the supernatant by impairing the assembly of infectious precursors in the ER.

Reduced apoB expression inhibits HCV assembly and secretion. Because impairment of MTP-dependent lipid transfer into apoB-containing pre-VLDL results in the inhibition of HCV particle assembly and secretion, we decided to study the impact of selective reduction of the intracellular levels of apoB on the HCV life cycle. It has been shown that shRNA-mediated downregulation of apoB expression reduces VLDL secretion in vitro (32) and in vivo (59). Taking advantage of this technology, we transduced Huh-7 cells with lentiviral vectors encoding two different shRNAs specific for apoB (32). As expected, expression of shRNAs 1 and 3 led to a stable reduction of apoB mRNA levels that led to reduced apoB secretion into the supernatant (Fig. 7A). This reduction was specific, since normal levels of human albumin were found in these supernatants (data not shown). Cells expressing the two shRNAs were infected with HCV at a low multiplicity (MOI of 0.01) to determine if reduced levels of apoB have a negative impact on viral spread. Viral spread was compromised in the cells that expressed reduced levels of apoB, as shown by the reduced number of infectious particles secreted into the supernatant over time (Fig. 7B). Interestingly, the reduction of viral titer observed at any given time point was proportional to the reduction of the secreted apoB level, as shown in Fig. 7A for the supernatants collected at day 7 postinfection. In similar infection experiments, chimeric viruses bearing structural proteins corresponding to genotype 1a (H77), genotype 1b (Con1), and genotype 2a (J6) showed a similar dependence on apoB for efficient infection (Fig. 7C and D). While these results are in good agreement with the hypothesis that HCV secretion is dependent on the cellular machinery responsible for VLDL secretion, other aspects of the viral life cycle could be affected by reduced apoB expression.

In order to define the role of apoB in the HCV life cycle, we performed single-cycle infection experiments with cells expressing shRNAs specific for apoB. apoB shRNA-transduced cells expressing low levels of apoB mRNA (Fig. 8A) were infected at an MOI of 5. Infected cells and their supernatants were collected at 24 and 48 h postinoculation, and intracellular and extracellular infectivity titers were determined as previously described (19). Figure 8B shows that the amount of infectious particles present in the supernatant of the infected cells was proportional to the level of secreted apoB, suggesting that apoB is rate limiting for HCV secretion (Fig. 8B). Extracellular HCV RNA levels were reduced accordingly (Fig. 8C), confirming that it is the reduction of secreted particles, not their infectivity, that is affected by reduced levels of apoB. Importantly, the levels of infectious intracellular particles were also reduced proportionally to the levels of apoB in the shRNA-expressing cells (Fig. 8B), suggesting that intracellular apoB levels determine the HCV particle assembly rate.

In order to discard the possibility that the reduced expression of apoB alters other aspects of the life cycle, such as infection efficiency or HCV RNA replication, we determined the intracellular levels of HCV RNA by RT-qPCR at 24 and 48 h postinfection. This analysis revealed that HCV RNA accumulation was comparable at 24 and 48 h, independently of apoB levels (Fig. 8D), suggesting that infection efficiency and HCV RNA replication remained unaffected in these cells. These results were confirmed by analyzing HCV RNA replication in cell lines bearing full-length and subgenomic JFH-1 replicons after transduction with lentiviruses encoding apoB shRNAs. In these cells, HCV RNA levels remained unaltered despite a significant reduction in apoB mRNA levels (Fig. 8E and F).

Overall, these results suggest that apoB is a cellular factor essential for the efficient assembly of infectious HCV particles and that the association of apoB with the mature HCV particles observed in infected patients might occur inside the infected cell.

DISCUSSION

A hallmark of HCV is that it circulates in the blood as a component of lipoproteins. Many reports suggest that HCV particles form complexes with VLDL components that circu-

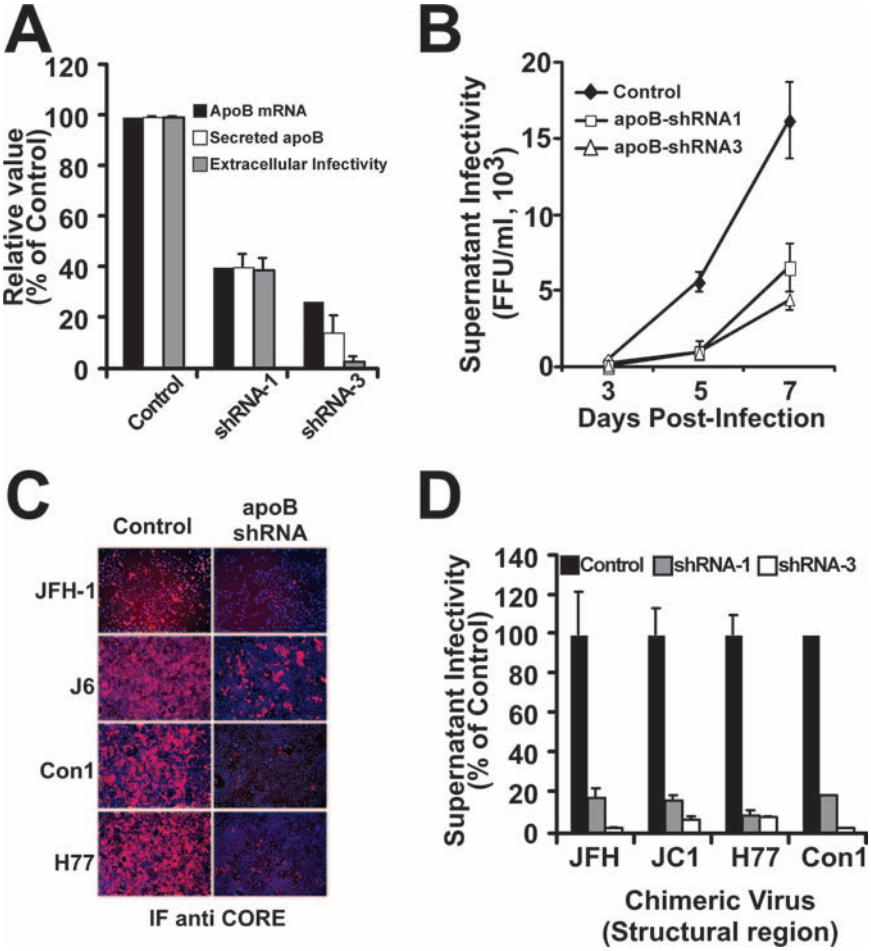

FIG. 7. Efficient HCV spread is impaired in cells expressing reduced apoB levels. apoB-deficient cells were infected at an MOI of 0.01 with JFH-1, and the infectivity in the cell supernatants was determined at different times postinfection. (A) apoB-deficient cells showed reduced apoB mRNA levels (black bars), as determined by RT-qPCR; reduced extracellular apoB levels (white bars), as determined by ELISA; and reduced HCV infectivity (gray bars) in the supernatants collected at day 7 postinfection. (B) Reduced cellular apoB levels lead to inefficient viral spread, as shown by the reduced numbers of infectious particles accumulated in the supernatant (FFU/ml) over time for cells expressing apoB shRNA-1 (white squares) and shRNA-3 (white triangles) compared to that for cells expressing GFP only (black diamonds). Results are presented as averages and standard deviations for duplicate experiments ($n = 2$). (C) apoB-deficient Huh-7 cells were infected at a low multiplicity (MOI of 0.01) with chimeric viruses expressing structural proteins from different genotypes. The reduced number of HCV core-positive cells at day 7 (JFH-1) or day 12 (J6, Con1, and H77) in apoB-deficient versus control cells suggests an inefficient viral spread in these cells, regardless of the genotype of the viral particles. (D) Infectivity titers at 7 days postinfection (FFU/ml) in the supernatants of cells infected at a low multiplicity reflect the reduced ability of cells expressing low apoB levels to produce infectious HCV particles from various HCV genotypes. Results are presented as percentages and are averages and standard deviations for triplicate experiments ($n = 3$).

late in infected patients (4). Recently, we and others showed that infectious HCV particles present in the supernatants of in vitro-infected hepatoma cell lines display a low-density profile similar to that described for the in vivo situation, suggesting that this association might also take place in vitro (19). We also showed that infectious HCV precursors display a different density profile, suggesting that their biochemical composition is different from that of secreted HCV virions (19). These results suggested that intracellular particles undergo a maturation process prior to their secretion, involving a biochemical transformation inside the infected cell, in a process in which the VLDL assembly and secretion machinery could be involved.

During preparation of the manuscript, a study carried out with surrogate models of HCV infection was published and suggested that assembly and secretion of HCV infectious particles are dependent on active secretion of VLDL (26). The present study provides a detailed dissection of the steps of the viral life cycle that intersect with the cellular VLDL secretion pathway during a complete HCV infection cycle in vitro. In this report, we used a specific MTP inhibitor and RNA interference to demonstrate that HCV coopts VLDL assembly and secretion for its own benefit. Specifically, apoB levels appear to be rate limiting for the assembly of infectious particles (Fig. 8B). Since apoB is translocated into the ER lumen as it is being translated, in a process facilitated by MTP (33), and since HCV core particles are believed to acquire the viral envelope by budding through the ER membrane (47), it is possible that apoB mediates this process or that apoB is acquired together with envelope proteins during the budding process. This would also explain the MTP dependency of HCV particle secretion

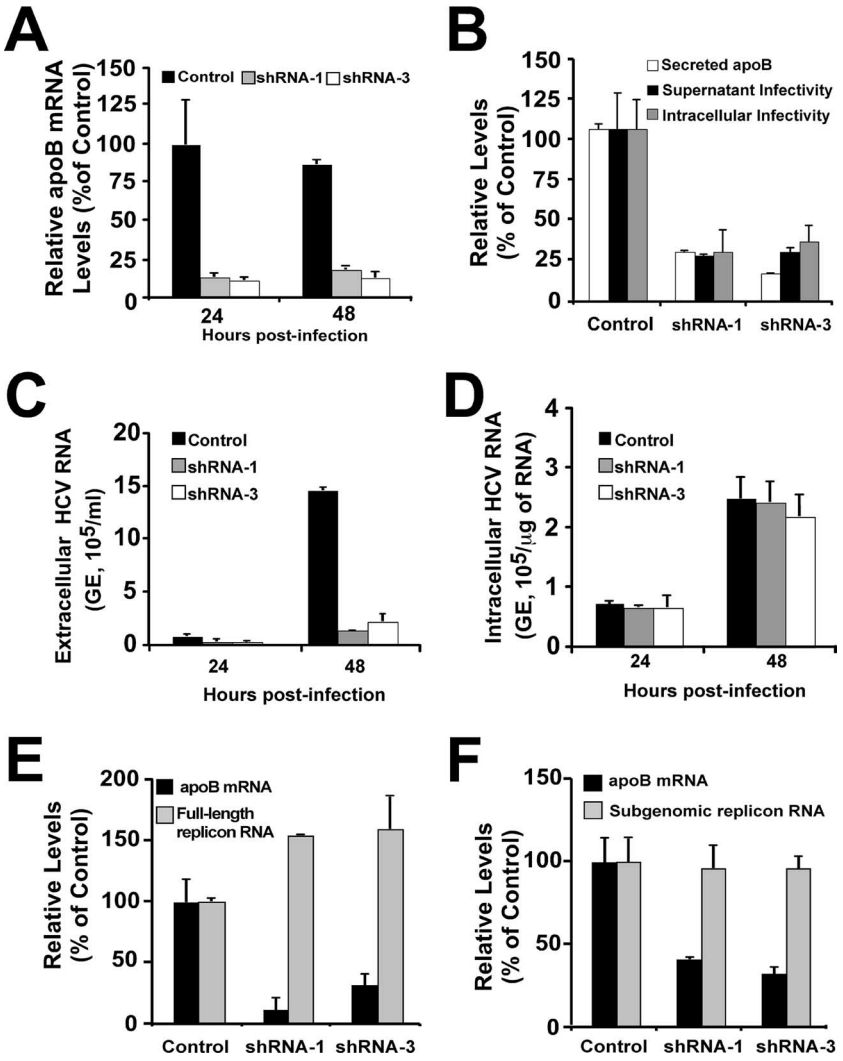

FIG. 8. Reduced apoB secretion reduces viral particle assembly and secretion without interfering with infection efficiency or HCV RNA replication. Cells expressing reduced apoB levels were infected at an MOI of 5 with a cell culture-adapted JFH-1 virus (see Materials and Methods). (A) Relative apoB mRNA quantitation by RT-qPCR shows a reduced expression of apoB in cells expressing specific shRNAs. Results are presented as percentages of the control level. (B) Infectivity titers determined at 24 h postinfection show a reduced accumulation of infectious HCV particles in the supernatant (black bars) as well as within infected cells (gray bars). This reduction was proportional to the level of secreted apoB (white bars). Results are presented as percentages of the control level. (C) Extracellular HCV RNA levels were also reduced in cells expressing the specific shRNA-1 (gray bars) and shRNA-3 (white bars) compared to that in the control cells (black bars), as determined by RT-qPCR. Results are shown as copy numbers/ml of supernatant. (D) Analysis of intracellular HCV RNA content by RT-qPCR revealed that there were no significant differences between control and shRNA-expressing cells at any time postinfection. Results are shown as copy numbers/μg of total cellular RNA. GE, genome equivalents. (E) Full-length JFH-1 replicon cells were transduced with lentiviral vectors expressing apoB shRNAs. The transduced cells were propagated, and HCV RNA as well as apoB mRNA levels were monitored by RT-qPCR. Results show HCV RNA levels when maximum apoB downregulation was observed (at 8 days posttransduction). (F) An identical experimental setup was used with cells bearing a subgenomic JFH-1 replicon. Results are presented as percentages and are averages and standard deviations for triplicate experiments ($n = 3$).

(Fig. 3), the low density of the secreted particles (19), and the presence of apoB in the particles circulating in infected patients (3, 42). Importantly, these observations apply to viruses expressing genotype 1a, 1b, and 2a structural proteins (Fig. 5E and 7C and D), suggesting that this is a general mechanism for HCV assembly and secretion. Although we provide evidence for a functional association between HCV and the VLDL secretion machinery, detailed biochemical analysis of the interactions between apoB and the viral structural proteins at different stages of the infection will be required to define the molecular mechanisms by which apoB determines HCV assembly and secretion.

We also observed that intracellular infectious particles or components essential for their assembly are degraded in a proteasome-independent manner. The rescue of functional, infectious particles by ALLN treatment (Fig. 3B and C) suggests that the viral and cellular components necessary for infectious particle assembly are properly folded and functional. This, together with the facts that this degradation is observed only when ER export is active (Fig. 3B) and that particle

secretion is not increased by ALLN treatment (Fig. 3D), suggests that the infectious particles themselves are targeted to degradation after they are assembled. The results presented in this study do not allow us to determine if accumulation of intracellular particles in the presence of ALLN and E64 reflects inhibition of a cysteine protease that directly degrades infectious HCV or that regulates HCV degradation by an indirect mechanism. Nevertheless, our results indicate that intracellular infectious HCV levels are regulated by a cysteine protease-dependent mechanism that does not affect virus particle secretion.

Overall, our results suggest that HCV assembly and secretion are part of a highly regulated process in which MTP-mediated translocation of apoB into the ER lumen is essential. While we speculate that the complex process that regulates the assembly and secretion of apoB-containing lipoproteins also regulates HCV assembly and secretion, our results suggest that high-density intracellular infectious HCV precursors undergo degradation by a nonproteasomal cysteine protease-dependent mechanism. In this context, we hypothesize that intracellular HCV precursors, which are assembled in the ER in an MTP-dependent manner, are targeted for degradation if they fail to undergo the biochemical maturation that is necessary for secretion (i.e., the addition of lipids). This hypothesis assumes that most of the assembled immature (i.e., high-density) HCV precursors are actively targeted for degradation in persistently infected cells. Although this concept seems counterintuitive, it suggests that a mechanism that selects a particular subset of viral particles (i.e., low-density particles) to be secreted may be in place. We can anticipate two possible advantages of this selection process. First, it is possible that diversion of the VLDL secretion machinery creates an intracellular environment that is optimal for the viral life cycle, i.e., by providing a lipid-rich intracellular environment (31) that facilitates virus assembly and secretion due to reduced lipid export (36, 40). Second, it is possible that the molecular anatomy of the particle selected for secretion confers an advantage over the immature infectious particles found in the cells, e.g., by masking viral envelope epitopes with host lipoproteins and limiting immune recognition in infected individuals or by providing cellular ligands permitting efficient binding to cellular coreceptors, such as SR-B1 (5, 29) or the LDL receptor (2).

ACKNOWLEDGMENTS

We thank the organizers of the 13th International Meeting on HCV and Related Viruses for providing us the opportunity of communicating these results ahead of publication. We thank Takaji Wakita (National Institute of Infectious Diseases, Tokyo, Japan) for kindly providing the infectious JFH-1 molecular clone and replicon constructs, Dennis Burton (Department of Immunology, The Scripps Research Institute. La Jolla, CA) for providing the recombinant human IgG anti-E2, Michael Houghton (Chiron, Emeryville, CA) for providing a polyclonal antibody against core HCV protein, I. Verma (Salk Institute, La Jolla, CA) for providing lentiviral plasmids, and Enrique Mann for synthesizing the MTP inhibitor (BMS-200150). We also thank Christina Whitten, Angelina Eustaquio, and Bryan Boyd for outstanding technical support.

This study was supported by grant R01-CA108304 from the National Institutes of Health and by a generous gift from Clifford Evans. This is manuscript number 18978 from the Scripps Research Institute.

REFERENCES

1. **Adeli, K.** 1994. Regulated intracellular degradation of apolipoprotein B in semipermeable HepG2 cells. J. Biol. Chem. **269:**9166–9175.
2. **Agnello, V., G. Abel, M. Elfahal, G. B. Knight, and Q. X. Zhang.** 1999. Hepatitis C virus and other Flaviviridae viruses enter cells via low density lipoprotein receptor. Proc. Natl. Acad. Sci. USA **96:**12766–12771.
3. **Andre, P., F. Komurian-Pradel, S. Deforges, M. Perret, J. L. Berland, M. Sodoyer, S. Pol, C. Brechot, G. Paranhos-Baccala, and V. Lotteau.** 2002. Characterization of low- and very-low-density hepatitis C virus RNA-containing particles. J. Virol. **76:**6919–6928.
4. **Andre, P., G. Perlemuter, A. Budkowska, C. Brechot, and V. Lotteau.** 2005. Hepatitis C virus particles and lipoprotein metabolism. Semin. Liver Dis. **25:**93–104.
5. **Bartosch, B., A. Vitelli, C. Granier, C. Goujon, J. Dubuisson, S. Pascale, E. Scarselli, R. Cortese, A. Nicosia, and F. L. Cosset.** 2003. Cell entry of hepatitis C virus requires a set of co-receptors that include the CD81 tetraspanin and the SR-B1 scavenger receptor. J. Biol. Chem. **278:**41624–41630.
6. **Baumert, T. F., S. Ito, D. T. Wong, and T. J. Liang.** 1998. Hepatitis C virus structural proteins assemble into virus-like particles in insect cells. J. Virol. **72:**3827–3836.
7. **Benoist, F., and T. Grand-Perret.** 1997. Co-translational degradation of apolipoprotein B100 by the proteasome is prevented by microsomal triglyceride transfer protein. Synchronized translation studies on HepG2 cells treated with an inhibitor of microsomal triglyceride transfer protein. J. Biol. Chem. **272:**20435–20442.
8. **Blasiole, D. A., R. A. Davis, and A. D. Attie.** 2007. The physiological and molecular regulation of lipoprotein assembly and secretion. Mol. Biosyst. **3:**608–619.
9. **Blight, K. J., A. A. Kolykhalov, and C. M. Rice.** 2000. Efficient initiation of HCV RNA replication in cell culture. Science **290:**1972–1975.
10. **Blight, K. J., J. A. McKeating, J. Marcotrigiano, and C. M. Rice.** 2003. Efficient replication of hepatitis C virus genotype 1a RNAs in cell culture. J. Virol. **77:**3181–3190.
11. **Brodsky, J. L., V. Gusarova, and E. A. Fisher.** 2004. Vesicular trafficking of hepatic apolipoprotein B100 and its maturation to very low-density lipoprotein particles; studies from cells and cell-free systems. Trends Cardiovasc. Med. **14:**127–132.
12. **Carabaich, A., M. Ruvoletto, E. Bernardinello, N. Tono, L. Cavalletto, L. Chemello, A. Gatta, and P. Pontisso.** 2005. Profiles of HCV core protein and viremia in chronic hepatitis C: possible protective role of core antigen in liver damage. J. Med. Virol. **76:**55–60.
13. **Chomczynski, P., and N. Sacchi.** 1987. Single-step method of RNA isolation by acid guanidinium thiocyanate-phenol-chloroform extraction. Anal. Biochem. **162:**156–159.
14. **Deleersnyder, V., A. Pillez, C. Wychowski, K. Blight, J. Xu, Y. S. Hahn, C. M. Rice, and J. Dubuisson.** 1997. Formation of native hepatitis C virus glycoprotein complexes. J. Virol. **71:**697–704.
15. **Duvet, S., L. Cocquerel, A. Pillez, R. Cacan, A. Verbert, D. Moradpour, C. Wychowski, and J. Dubuisson.** 1998. Hepatitis C virus glycoprotein complex localization in the endoplasmic reticulum involves a determinant for retention and not retrieval. J. Biol. Chem. **273:**32088–32095.
16. **Fisher, E. A., M. Pan, X. Chen, X. Wu, H. Wang, H. Jamil, J. D. Sparks, and K. J. Williams.** 2001. The triple threat to nascent apolipoprotein B. Evidence for multiple, distinct degradative pathways. J. Biol. Chem. **276:**27855–27863.
17. **Friebe, P., and R. Bartenschlager.** 2002. Genetic analysis of sequences in the 3′-nontranslated region of hepatitis C virus that are important for RNA replication. J. Virol. **76:**5326–5338.
18. **Friebe, P., J. Boudet, J. P. Simorre, and R. Bartenschlager.** 2005. Kissing-loop interaction in the 3′ end of the hepatitis C virus genome essential for RNA replication. J. Virol. **79:**380–392.
19. **Gastaminza, P., S. B. Kapadia, and F. V. Chisari.** 2006. Differential biophysical properties of infectious intracellular and secreted hepatitis C virus particles. J. Virol. **80:**11074–11081.
20. **Gibbons, G. F., D. Wiggins, A. M. Brown, and A. M. Hebbachi.** 2004. Synthesis and function of hepatic very-low-density lipoprotein. Biochem. Soc. Trans. **32:**59–64.
21. **Gordon, D. A., H. Jamil, R. E. Gregg, S. O. Olofsson, and J. Boren.** 1996. Inhibition of the microsomal triglyceride transfer protein blocks the first step of apolipoprotein B lipoprotein assembly but not the addition of bulk core lipids in the second step. J. Biol. Chem. **271:**33047–33053.
22. **Gusarova, V., J. L. Brodsky, and E. A. Fisher.** 2003. Apolipoprotein B100 exit from the endoplasmic reticulum (ER) is COPII-dependent, and its lipidation to very low density lipoprotein occurs post-ER. J. Biol. Chem. **278:**48051–48058.
23. **Heller, T., S. Saito, J. Auerbach, T. Williams, T. R. Moreen, A. Jazwinski, B. Cruz, N. Jeurkar, R. Sapp, G. Luo, and T. J. Liang.** 2005. An in vitro model of hepatitis C virion production. Proc. Natl. Acad. Sci. USA **102:**2579–2583.
24. **Honda, M., M. R. Beard, L. H. Ping, and S. M. Lemon.** 1999. A phylogenetically conserved stem-loop structure at the 5′ border of the internal ribosome entry site of hepatitis C virus is required for cap-independent viral translation. J. Virol. **73:**1165–1174.

25. **Hoofnagle, J. H.** 2002. Course and outcome of hepatitis C. Hepatology **36:**S21–S29.
26. **Huang, H., F. Sun, D. M. Owen, W. Li, Y. Chen, M. Gale, Jr., and J. Ye.** 2007. Hepatitis C virus production by human hepatocytes dependent on assembly and secretion of very low-density lipoproteins. Proc. Natl. Acad. Sci. USA **104:**5848–5853.
27. **Jamil, H., D. A. Gordon, D. C. Eustice, C. M. Brooks, J. K. Dickson, Jr., Y. Chen, B. Ricci, C. H. Chu, T. W. Harrity, C. P. Ciosek, Jr., S. A. Biller, R. E. Gregg, and J. R. Wetterau.** 1996. An inhibitor of the microsomal triglyceride transfer protein inhibits apoB secretion from HepG2 cells. Proc. Natl. Acad. Sci. USA **93:**11991–11995.
28. **Kafri, T., U. Blomer, D. A. Peterson, F. H. Gage, and I. M. Verma.** 1997. Sustained expression of genes delivered directly into liver and muscle by lentiviral vectors. Nat. Genet. **17:**314–317.
29. **Kapadia, S. B., H. Barth, T. Baumert, J. A. McKeating, and F. V. Chisari.** 2007. Initiation of hepatitis C virus infection is dependent on cholesterol and cooperativity between CD81 and scavenger receptor B type I. J. Virol. **81:**374–383.
30. **Kapadia, S. B., A. Brideau-Andersen, and F. V. Chisari.** 2003. Interference of hepatitis C virus RNA replication by short interfering RNAs. Proc. Natl. Acad. Sci. USA **100:**2014–2018.
31. **Kapadia, S. B., and F. V. Chisari.** 2005. Hepatitis C virus RNA replication is regulated by host geranylgeranylation and fatty acids. Proc. Natl. Acad. Sci. USA **102:**2561–2566.
32. **Liao, W., and G. Ning.** 2006. Knockdown of apolipoprotein B, an atherogenic apolipoprotein, in HepG2 cells by lentivirus-mediated siRNA. Biochem. Biophys. Res. Commun. **344:**478–483.
33. **Liao, W., S. C. Yeung, and L. Chan.** 1998. Proteasome-mediated degradation of apolipoprotein B targets both nascent peptides cotranslationally before translocation and full-length apolipoprotein B after translocation into the endoplasmic reticulum. J. Biol. Chem. **273:**27225–27230.
34. **Lindenbach, B. D., H.-J. Thiel, and C. M. Rice.** 2001. *Flaviviridae*: the viruses and their replication, p. 1101–1152. *In* D. M. Knipe, P. M. Howley, D. E. Griffin, R. A. Lamb, M. A. Martin, B. Roizman, and S. E. Straus (ed.), Fields virology, 5th ed., vol. 2. Lippincott Williams & Wilkins, Philadelphia, PA.
35. **Lohmann, V., F. Korner, J. Koch, U. Herian, L. Theilmann, and R. Bartenschlager.** 1999. Replication of subgenomic hepatitis C virus RNAs in a hepatoma cell line. Science **285:**110–113.
36. **Lonardo, A., L. E. Adinolfi, P. Loria, N. Carulli, G. Ruggiero, and C. P. Day.** 2004. Steatosis and hepatitis C virus: mechanisms and significance for hepatic and extrahepatic disease. Gastroenterology **126:**586–597.
37. **Macovei, A., N. Zitzmann, C. Lazar, R. A. Dwek, and N. Branza-Nichita.** 2006. Brefeldin A inhibits pestivirus release from infected cells, without affecting its assembly and infectivity. Biochem. Biophys. Res. Commun. **346:**1083–1090.
38. **Mizuno, M., G. Yamada, T. Tanaka, K. Shimotohno, M. Takatani, and T. Tsuji.** 1995. Virion-like structures in HeLa G cells transfected with the full-length sequence of the hepatitis C virus genome. Gastroenterology **109:** 1933–1940.
39. **Moradpour, D., R. Gosert, D. Egger, F. Penin, H. E. Blum, and K. Bienz.** 2003. Membrane association of hepatitis C virus nonstructural proteins and identification of the membrane alteration that harbors the viral replication complex. Antivir. Res. **60:**103–109.
40. **Napolitano, M., A. Giuliani, T. Alonzi, C. Mancone, G. D'Offizi, M. Tripodi, and E. Bravo.** 2007. Very low density lipoprotein and low density lipoprotein isolated from patients with hepatitis C infection induce altered cellular lipid metabolism. J. Med. Virol. **79:**254–258.
41. **Nebenfuhr, A., C. Ritzenthaler, and D. G. Robinson.** 2002. Brefeldin A: deciphering an enigmatic inhibitor of secretion. Plant Physiol. **130:**1102–1108.
42. **Nielsen, S. U., M. F. Bassendine, A. D. Burt, C. Martin, W. Pumeechockchai, and G. L. Toms.** 2006. Association between hepatitis C virus and very-low-density lipoprotein (VLDL)/LDL analyzed in iodixanol density gradients. J. Virol. **80:**2418–2428.
43. **Patel, K., and J. G. McHutchison.** 2004. Initial treatment for chronic hepatitis C: current therapies and their optimal dosing and duration. Cleve. Clin. J. Med. **71**(Suppl. 3)**:**S8–S12.
44. **Penin, F., J. Dubuisson, F. A. Rey, D. Moradpour, and J. M. Pawlotsky.** 2004. Structural biology of hepatitis C virus. Hepatology **39:**5–19.
45. **Pietschmann, T., A. Kaul, G. Koutsoudakis, A. Shavinskaya, S. Kallis, E. Steinmann, K. Abid, F. Negro, M. Dreux, F. L. Cosset, and R. Bartenschlager.** 2006. Construction and characterization of infectious intragenotypic and intergenotypic hepatitis C virus chimeras. Proc. Natl. Acad. Sci. USA **103:**7408–7413.
46. **Pumeechockchai, W., D. Bevitt, K. Agarwal, T. Petropoulou, B. C. Langer, B. Belohradsky, M. F. Bassendine, and G. L. Toms.** 2002. Hepatitis C virus particles of different density in the blood of chronically infected immunocompetent and immunodeficient patients: implications for virus clearance by antibody. J. Med. Virol. **68:**335–342.
47. **Roingeard, P., C. Hourioux, E. Blanchard, D. Brand, and M. Ait-Goughoulte.** 2004. Hepatitis C virus ultrastructure and morphogenesis. Biol. Cell **96:**103–108.
48. **Rouille, Y., F. Helle, D. Delgrange, P. Roingeard, C. Voisset, E. Blanchard, S. Belouzard, J. McKeating, A. H. Patel, G. Maertens, T. Wakita, C. Wychowski, and J. Dubuisson.** 2006. Subcellular localization of hepatitis C virus structural proteins in a cell culture system that efficiently replicates the virus. J. Virol. **80:**2832–2841.
49. **Rustaeus, S., K. Lindberg, P. Stillemark, C. Claesson, L. Asp, T. Larsson, J. Boren, and S. O. Olofsson.** 1999. Assembly of very low density lipoprotein: a two-step process of apolipoprotein B core lipidation. J. Nutr. **129:**463S–466S.
50. **Rustaeus, S., P. Stillemark, K. Lindberg, D. Gordon, and S. O. Olofsson.** 1998. The microsomal triglyceride transfer protein catalyzes the post-translational assembly of apolipoprotein B-100 very low density lipoprotein in McA-RH7777 cells. J. Biol. Chem. **273:**5196–5203.
51. **Sasaki, T., M. Kishi, M. Saito, T. Tanaka, N. Higuchi, E. Kominami, N. Katunuma, and T. Murachi.** 1990. Inhibitory effect of di- and tripeptidyl aldehydes on calpains and cathepsins. J. Enzyme Inhib. **3:**195–201.
52. **Siagris, D., M. Christofidou, G. J. Theocharis, N. Pagoni, C. Papadimitriou, A. Lekkou, K. Thomopoulos, I. Starakis, A. C. Tsamandas, and C. Labropoulou-Karatza.** 2006. Serum lipid pattern in chronic hepatitis C: histological and virological correlations. J. Viral Hepat. **13:**56–61.
53. **Sparks, J. D., T. L. Phung, M. Bolognino, and C. E. Sparks.** 1996. Insulin-mediated inhibition of apolipoprotein B secretion requires an intracellular trafficking event and phosphatidylinositol 3-kinase activation: studies with brefeldin A and wortmannin in primary cultures of rat hepatocytes. Biochem. J. **313:**567–574.
54. **Su, A. I., J. P. Pezacki, L. Wodicka, A. D. Brideau, L. Supekova, R. Thimme, S. Wieland, J. Bukh, R. H. Purcell, P. G. Schultz, and F. V. Chisari.** 2002. Genomic analysis of the host response to hepatitis C virus infection. Proc. Natl. Acad. Sci. USA **99:**15669–15674.
55. **Ye, S. Q., C. A. Reardon, and G. S. Getz.** 1993. Inhibition of apolipoprotein E degradation in a post-Golgi compartment by a cysteine protease inhibitor. J. Biol. Chem. **268:**8497–8502.
56. **Yeung, S. J., S. H. Chen, and L. Chan.** 1996. Ubiquitin-proteasome pathway mediates intracellular degradation of apolipoprotein B. Biochemistry **35:** 13843–13848.
57. **Zhong, J., P. Gastaminza, G. Cheng, S. Kapadia, T. Kato, D. R. Burton, S. F. Wieland, S. L. Uprichard, T. Wakita, and F. V. Chisari.** 2005. Robust hepatitis C virus infection in vitro. Proc. Natl. Acad. Sci. USA **102:**9294–9299.
58. **Zhong, J., P. Gastaminza, J. Chung, Z. Stamataki, M. Isogawa, G. Cheng, J. A. McKeating, and F. V. Chisari.** 2006. Persistent hepatitis C virus infection in vitro: coevolution of virus and host. J. Virol. **80:**11082–11093.
59. **Zimmermann, T. S., A. C. Lee, A. Akinc, B. Bramlage, D. Bumcrot, M. N. Fedoruk, J. Harborth, J. A. Heyes, L. B. Jeffs, M. John, A. D. Judge, K. Lam, K. McClintock, L. V. Nechev, L. R. Palmer, T. Racie, I. Rohl, S. Seiffert, S. Shanmugam, V. Sood, J. Soutschek, I. Toudjarska, A. J. Wheat, E. Yaworski, W. Zedalis, V. Koteliansky, M. Manoharan, H. P. Vornlocher, and I. MacLachlan.** 2006. RNAi-mediated gene silencing in non-human primates. Nature **441:**111–114.